AUTOFLUORESCENCE AREAS DETECTION IN HRA IMAGES

R. Kolář*, J. Jan*, R. Chrástek**, R. Laemmer***, Ch. Y. Mardin***

*Department of Biomedical Engineering, FEEC, Brno University of Technology,
Brno, Czech Republic

**Department of Computer Science, Friedrich-Alexander University
of Erlangen-Nürnberg, Germany

***Department of Ophthalmology, Friedrich-Alexander University
of Erlangen-Nürnberg, Germany

kolarr@feec.vutbr.cz

Abstract: We present a semi-automatic and a fully automatic method for detection of lipofuscin accumulation zones in autofluorescent images of retina. It is believed that these zones are important in diagnostic process of glaucoma and other ophthalmological changes. We use region growing method and active contour model in connection with some basic image processing methods.

Keywords: image segmentation, retina, region growing, active contour

Introduction

The Heidelberg Retina Angiograph (HRA2, Heidelberg Retina Angiograph) is a kind of scanning laser ophthalmoscope used for angiographic examination of human retina. There are several modes of examination, e.g. fluorescein angiography, ICG angiography, infra-red imaging [5]. Images that we are interested in are obtained in autofluorescent (AF) mode and have the resolution 10μm/pixel and size 512x512 pixels.

In this mode, the retina is illuminated by a narrow blue laser light beam (λ=488 nm) in a raster manner. This beam excites the lipofuscin that emits light with longer wavelength (around 500nm) [4]. The emission intensity depends on the amount of lipofuscin accumulation in retinal pigment epithelium (RPE). We are focused on these AF zones of lipofuscin because there are some studies showing the correlation between lipofuscin accumulation around the optic disc (OD) with the stage of optic disc atrophy [1]. Parapapillary autofluorescence is predominantly observed at the border of atrophic zone alpha. Histological and electron microscopic investigations demonstrate an accumulation of lipofuscin in lysosomes of the retinal pigment epithelium in this region [13]. Clinically parapapillary atrophic zone alpha is characterized by hyper- and hypopigmentation. Histologically vacuoles, cell atrophy and lipofuscin accumulation can be recognized beside an inhomogeneous distribution of melanin granules in the retinal pigment epithelium, whereas parapapillary atrophic zone beta shows complete loss of retinal pigment epithelium as well as marked reduction of photoreceptors and rarificaction of chorioidal vessels [11, 12, 13]. Progression of parapapillary atrophic zone beta (atrophic zone alpha turns into beta) is correlated with progression of the morphologic [11, 14] and functional [15, 16] glaucomatous damage. Measurement of time resolution autofluorescence using lifetime images from single photon counting [17] identified also lipofuscin in the parapapillary region [18]. Histopathological studies have also shown that accumulation of lipofuscin in the RPE is an early feature indicating some disorders at the time when other ophthalmologic changes are absent [4].

Therefore, the detection of active parapapillary AF areas especially in case of ocular hypertension (and possibly glaucoma) may offer an important tool for early diagnosis [1]. It has been shown that some geometric parameters (shape, distance and area) of these AF zones can assist the glaucoma diagnosis [1]. Standard HRA software allows quantitative assessment, but image analysis requires manual outlining of interested structures. This is subjective to a certain degree. Intraobserver variability has shown to be relatively low, but interobserver variability is limited even if assessment is performed by experienced ophthalmologists. Hence our contribution focused on the semi – automatic and possibly also fully automatic AF zones segmentation.

Method

Our aim is to detect the areas with lipofuscin accumulation (*AF zones*). Once we know the position of the pixels that belong to the particular zones, we can determine zone parameters for diagnosis (area, distance from optical disc (OD) and other shape parameters [1]). The importance of these parameters in diagnostic process is not clear yet and will be in the range of our

ISSN: 1727-1983

interest in near future. Here we are focused only on AF zones segmentation.

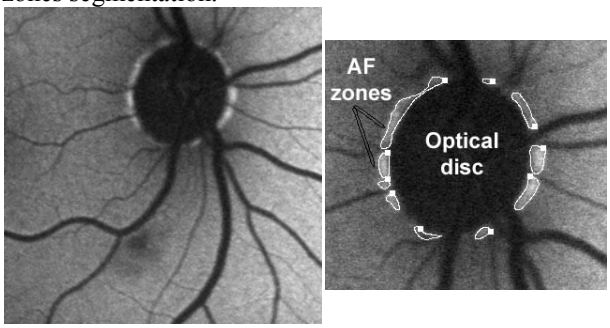

Figure 1: The AF image and a detail of the optical disc surroundings. The AF zones are visible as bright areas around the black spot

Figure 1 shows the close surroundings of the optical disc (OD) with manually segmented AF zones. In fact, the border of the dark area is not the true OD border as can be seen for example in fundus images. Inside this black spot in AF images is zone beta, which doesn't contain any AF zone [1]. This zone is peripapillary crescent mostly in the temporal region or circular in more advanced stages. Parapapillary atrophic zone beta is attached to the scleral ring of Elschnig, which represent the optic disc border, and toward the periphery followed by zone alpha. On fundus color photography zone beta appears as grey field on a whitish background, with good visibility of large choroidal vessels due to atrophy of retinal pigment epithelium, thinning of chorioretinal tissues and rarificaction of chorioidal vessels [11]. The circular extension of AF surrounding the OD is about 0.5 mm, but in cases with advanced glaucomatous damage this distance is on average 2,4 mm and can reach up to more than 5 mm. The typical area ranges from 0.05 mm² in normals to 0.24 mm² in early and 0.46 mm² in advanced glaucomas [1]. The aim of our work is to semi automatically or fully automatically determines the borders of the all AF zones in measured image. We have at disposal AF image database with 20 manually segmented images.

First, we will present the *semi-automatic method*, which is based on the interactive indication of point (a seed) inside each AF area. This method can be divided into 4 steps:
1.image preprocessing;
2.manual indication of seed point;
3.applying region growing;
4.fine adjustment of the detected contour based on human decision (increasing or decreasing contour, applying active contour approach);

As can be seen from Figure 1, the AF images are quite noisy, although this image is a result of averaging of several images obtained by HRA2 [10]. As a preprocessing step, a simple median filter is used. The size of this window ([5x5] pixels) was determined based on analysing the minimal size of AF zone in our database.

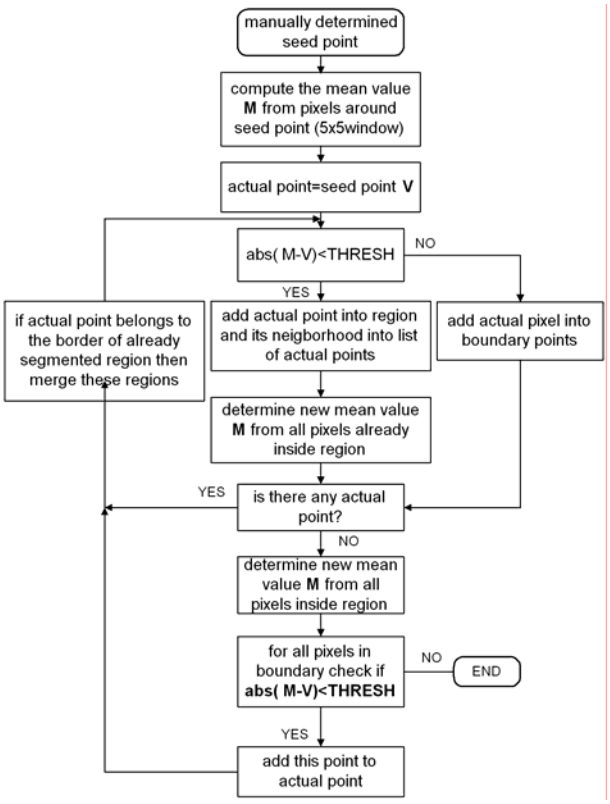

Figure 2: Algorithm for semi-automatic method

The heart of this segmentation lies in the region growing method. Even though the principle of this method is clear [5], it must be adjusted for a particular application. For AF area detection we use the fact that the pixels inside this area have higher intensity than surrounding pixels (see example on Fig.1). Therefore, the decision rule (i.e. if actual pixel belongs into the region or not) is based on the pixel intensity value and the mean instantaneous value of the actual region that is changing during the growing process. The whole algorithm is depicted on Fig.2. One important parameter of this method is the threshold THRESH that influence the sensitivity of this method.

Some images segmented by this semi automatic approach are depicted on Fig. 3. The seed points were indicated manually – one for each AF zone. After this segmentation process, the user can adjust the contour by extending or shrinking (Figure 4). The application of active contour approach is also possible and will be explained later.

Our further aim is to develop a *fully automated AF zone segmentation method*. The AF images have various illuminations within the whole image. Therefore, it is hard to determine some reasonable threshold for simple segmentation by thresholding. To cope with this negative property, we would like to determine the region of interest (ROI) only. This ROI contains the structures near the optic disc (the dark spot). Because this spot has a dark color in all images in our database, we can do simple thresholding with a predefined

ISSN: 1727-1983

threshold determined experimentally by analysing AF images.

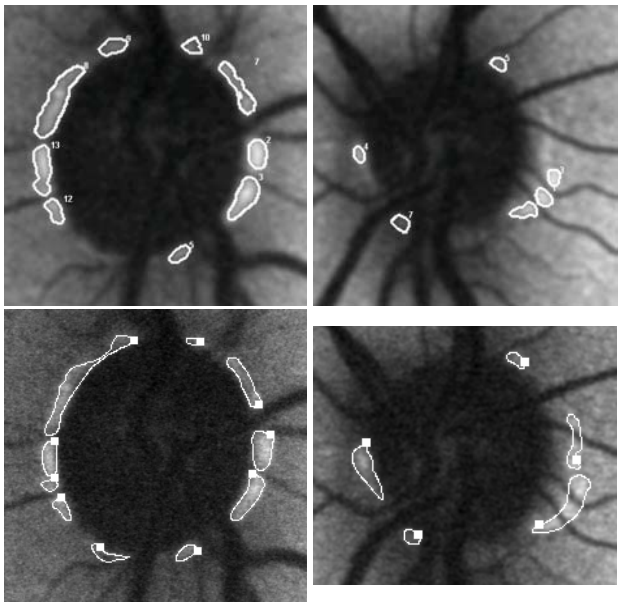

Figure 3: Segmented images by semi-automatic method (first row) and corresponding manually segmented images (second row)

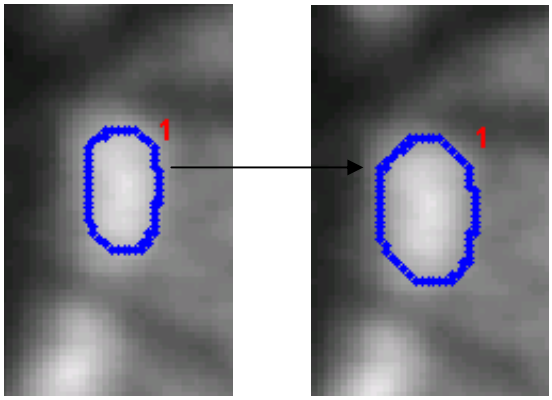

Figure 4: Extension of the detected contour by morphologic increasing. Each pixel of boundary is moved out, with respect to the centre of region

We have also tested one automatic thresholding method - Otsu method, which finds the threshold by minimizing the within-group variance [3] and the threshold had to be decreased for every image by multiplying by some value. See Figure 5b for the result after thresholding. We would like to detect the region around the black spot. To remove the vascular structure some morphology operation [5, 7] was performed. Image erosion with line structure element of length 10 pixels (100μm) and equally spaced angle (15°) were used. These operations successfully removed the blood vessels and preserved the OD (Figure 5c). Once we have the optic disc border, we can extend this region by some length. The extent is determined by the maximum distance between lipofuscin accumulation and OD border, which has been found to correspond to 50 pixels. The resulted region of interest is on Figure 5d.

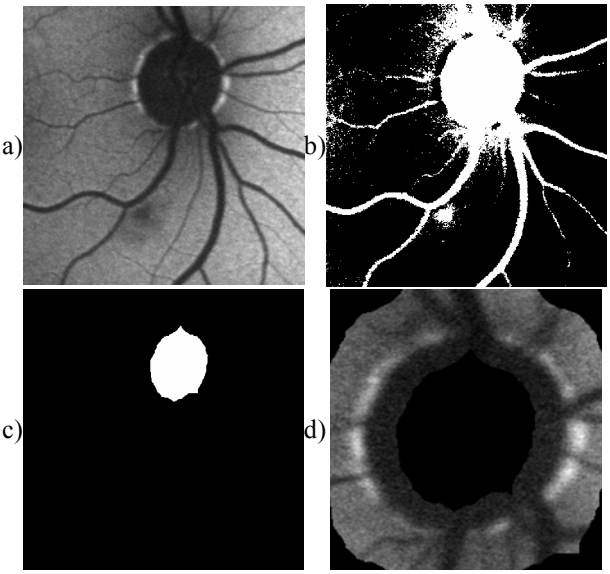

Figure 5: Segmentation of ROI. a) original image, b) thresholded image, c) OD segmentation, d) segmented ROI

The next step is to find the seed points for region growing. We used the thresholding technique again, applied only on the segmented ROI. An example of thresholded ROI is on Figure 6a. Each white region is automatically marked; the contour of each region is found and used as a boundary for region growing described above. The example result is depicted on Figure 6b; corresponding image is on Figure 3 (left). One can see that in the automatically segmented image, some AF areas are not found due to the low numbers of initial seed points (low sensitivity).

The *active contour* (snake, deformable model) was tested for AF zone modification. The reason for using snakes is to make a fine adjustment of contour detected by region growing. It is based on mutual compensation of external and internal forces. A traditional 2D snake is a curve $x(s) = [x(s), y(s)]$, $s \in [0,1]$, that deforms and moves through the spatial domain of an image to minimize the energy functional [6]:

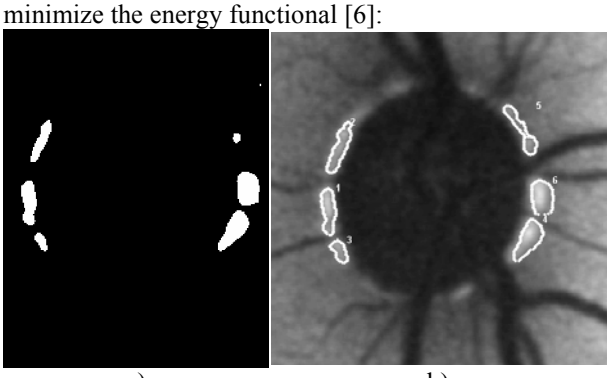

a) b)

Figure 6: Automatically detected seed points for region growing (a) and the result (b). Corresponding image is on Figure 3 (left)

ISSN: 1727-1983

$$E = \int_0^1 \frac{1}{2}\left(\alpha\left|x'(s)\right|^2 + \beta\left|x''(s)\right|^2\right) + E_{ext}\left(x(s)\right) ds\,, \quad (1)$$

where α and β are weighting parameters that control the deformable contour tension and rigidity, respectively. *x'(s)* and *x''(s)* denote the first and second derivatives with respect to *s*. The E_{ext} is an external force field – typically the (smoothed) derivative of the image or more advanced function, e.g. GVF [6]. In our application this force field is obtained as a weighted sum of smoothed image gradient and distance transform [8] gradient:

$$E_{ext} = k.grad(L) + (1-k).grad(D)\,, \quad (2)$$

where *L* is the intensity image, *D* is the distance transform of this image and *k* is parameter that influences the sensitivity of snakes. We observed that combination of these gradients could give a satisfactory result better than the simple image gradient. The value of the parameter *k* has been found around *0.1*.

Besides the snake parameters α, β and E_{ext}, snakes are sensitive to initial contour shape, which was provided with the help of region growing method by taking several node points from the borders of each region (see Figure 8a). Whole application described on the flow chart, on Figure 7. The snake's algorithm was implemented by Xu and colleagues, can be obtained through the www [9].

Results and Conclusion

Evaluation of the proposed algorithm is quite complicated because there is a high inter-operator variability in delineation of AF zones between physicians. Also our database contains only 20 images, so that a quantitative evaluation wouldn't be reliable. So far, we can make only some conclusions based on the experiences with the developed application software (under Matlab).

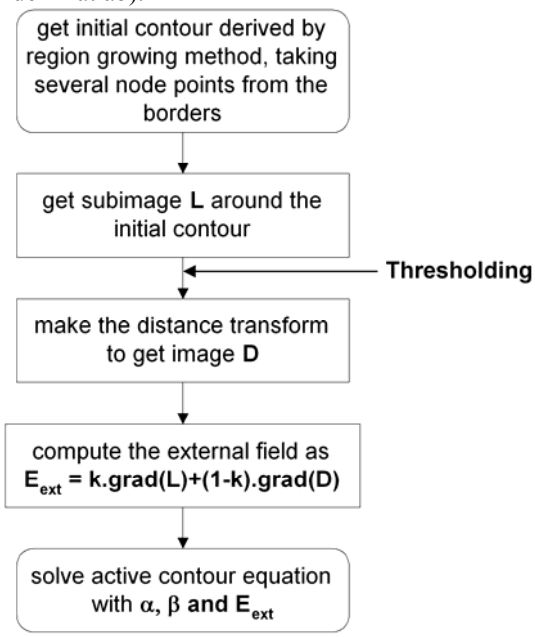

Figure 7: Flow chart for application of active contour

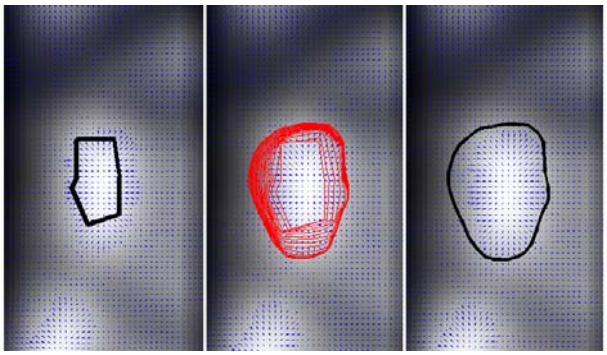

a) b) c)

Figure 8: Application of snakes: a) initialization curve based on region growing; b) the curve evolution; c) the resulting contour. The grey arrows show the external force field

The advantage of semiautomatic segmentation over full automatic segmentation and manual delineation is that it is not so much sensitive on operator placement of the seed points. This is because the operator places the seed point 'somewhere' and the maximum intensity point in its neighbourhood is taken as a 'true' seed point. The success of segmentation depends on the parameter THRESH that influences the sensitivity. Too low (too high) parameter will stop the growing process too early (too late). According to our experiment, it is better to set this parameter to a lower level (about 15) and then to use the active contour to make a fine adjustment of the region contour.

The fully automatic process is not successful for all images, because there is high illumination variability between AF images. This needs some kind of background extraction, possibly based on histogram analysis. This is one of the aims in a near future, which is expected to improve the seed point sensitivity. But the main problem is the high inter-operator variability.

Although most information is obviously included in brightness, the detailed texture analysis will be the next step in the near future.

Acknowlegments

This work has been supported by the grant no. 102/03/P153 of Czech Science Foundation and by the Research center no. 1M679855501 under Ministry of Education (Czech Republic).

The authors would like to thank to Dr. Arne Viestenz, Dr. Robert Lämmer and Priv. Doz. Dr. Christian Mardin (Augenklink, Universitätseklinikum Erlangen, Germany) for their valuable comments and for providing the image data.

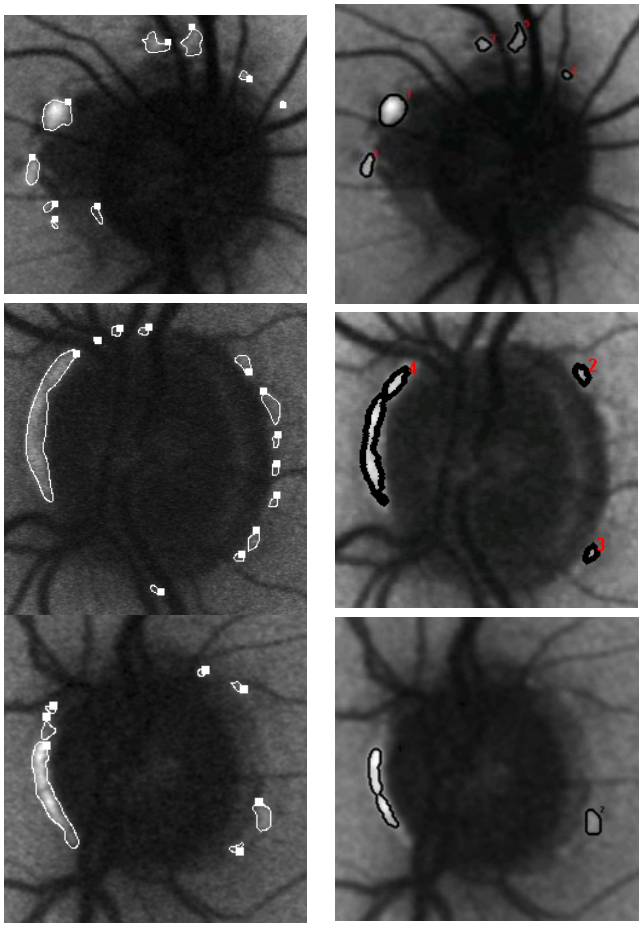

a) b)

Figure 9: Sample results of a) manually segmented images and b) results of semi automated detection

References

[1] VIESTENZ, A. ET AL. (2003): „In-vivo-Messung der Autofluoreszenz in der parapapillaren Atrophiezone bei Papillen mit und ohne glaukomatose Optikusatrophie“, Klin Monatssbl Augenheilkd 2003, **220**, pp. 545 - 550

[2] Xu C., Prince J. L. (1997): "Gradient Vector Flow: A New External Force for Snakes", *IEEE Proc. Conf. on Comp. Vis. Patt. Recog.* (CVPR'97), pp. 66-71

[3] AZHAR H., WIDJANARKO T. (2002): “Comparison of Two Binary Image Threholding Methods”, Final project paper, EECE Department, University of Memphis.

[4] RUCKMANN A., FITZKE W.F., BIRD A.C. (1995): “Distribution of Fundus Autofluorescence with a Scanning Laser Ophthalmoscope”, *Journal of Ophthalmology*, **79**, pp. 407 – 412

[5] JAIN, A.. K. (1988): “Fundamentals of Digital Image Processing”, Prentice Hall

[6] BANKMAN I. N. (2000): “Handbook of Medical Imaging”, Academic Press, pp. 159-169

[7] GONZALES R.C., WINTZ P. (1987): ‘Digital image processing’, Addison-Wesley

[8] HIPR - Hypermedia Image Processing Reference, Internet Site address: http://www.cee.hw.ac.uk/hipr/html

[9] GVF code, Internet Site address: http://iacl.ece.jhu.edu/projects/gvf/

[10] HRA2 information, Internet Site address: http://www.heidelbergengineering.com/

[11] JONAS J.B., NGUYEN X.N., GUSEK G.C. et al. (1989): “Parapapillary chorioretinal atrophy in normal and glaucoma eyes”, Invest Ophthalmol Vis Sci, **30**, pp. 908 - 918

[12] KUBOTA T., JONAS J.B., NAUMANN G.O.H. (1993): “Direct clinico-histological correlation of parapapillary chorioretinal atrophy”, Br J Ophthalmol, **77**, pp. 103 - 106

[13] KUBOTA T., SCHLÖTZER-SCHREHARDT U.M., NAUMANN G.O.H. et al. (1996): “The ultrastructure of parapapillary chorioretinal atrophy in eyes with secondary angle closure glaucoma”, Graefes Arch Clin Exp Ophthalmol, **234**, pp. 351 - 358

[14] ROCKWOOD E.J., ANDERSON D.R. (1988): “Acquired peripapillary changes and progression in glaucoma”, Graefes Arch Clin Exp Ophthalmol, **226**, pp. 510 - 515

[15] JONAS J.B., GRUNDLER A.E. (1997): “Correlation between mean visual field loss and morphometric optic disk variables in the open-angle glaucomas”, Am J Ophthalmol, **124,** pp. 488 - 497

[16] KONO Y., ZANGWILL L., SAMPLE P.A. et al. (1999): “Relationship between parapapillary atrophy and visual field abnormality in primary open-angle glaucoma”, Am J Ophthalmol, **127**, pp. 674 - 680

[17] SCHWEITZER D., HAMMER M., SCHWEITZER F. et al. (2004): „In vivo measurement of time-resolved autofluorescence at the human fundus”, J Biomed Opt, **9**, pp. 1214 - 1222

[18] SCHWEITZER D., KOLB A., HAMMER M. et al. (2002): „Time-correlated measurement of autofluorescence. A method to detect metabolic changes in the fundus”, Ophthalmologe, **99**, pp.774 - 779

ISSN: 1727-1983